Universität Hamburg
DER FORSCHUNG | DER LEHRE | DER BILDUNG

Deutsches Klimarechenzentrum (DKRZ) User Workshop
Hamburg, 26 February 2013

cen

bu0450: North Atlantic key processes investigated with high-resolution data assimilation

N. Serra, A. Köhl & D. Stammer, Institut für Meereskunde, CEN, University of Hamburg, Germany

1. Introduction

A dynamically consistent description of the **2000-2010** North Atlantic circulation and associated surface forcing fields was obtained through **model-data synthesis using the adjoint method** at an eddy-permitting/resolving resolution (16 km).

The method is a **4-dimensional variational data assimilation** method (4DVAR), consisting on a minimization (the observations-model misfit) subject to a strong constraint: the sequence of model states is a solution of the model equations (this prevents jumps in the solution). The overall procedure, repeated until convergence towards the "true" state, is (Fig. 1):

- non-linear model is integrated forward (first-guess) and mismatches between simulation and all measurements is computed (global cost function).
- adjoint of the linearized model computes gradients of cost function with respect to all control variables.
- descent algorithm finds corrections to control variables leading to a model path that globally reduces the cost.
- improved simulation is run subject to the improved controls, i.e., initial and boundary conditions.

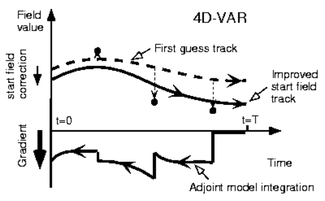

Fig. 1. *4D variational data assimilation.*

2. High-resolution ocean synthesis

The **assimilated observational data** were:
- monthly temperature and salinity profiles from CTDs, XBTs and ARGO floats;
- daily along-track sea surface height (SSH) anomalies from satellite altimetry;
- monthly sea surface temperatures (SST) from satellite microwave sensor.

The variables modified (every 3 days) to achieve model-observations consistency (the **controls**) were:
- initial temperature and salinity conditions;
- surface boundary conditions: 2-m air temperature and humidity, precipitation, 10-m wind.

The 2000-2010 **model-observations misfit reduced by about 40%** (after 9 iterations). Largest individual cost reductions occurred for salinity (37%) and temperature (17%). Small improvement in SSH was obtained, since the forward integration SSH was already near accepted errors. It might also indicate that constraining eddy variability of an already eddying model is problematic.

Bias reduction for salinity and temperature (Fig. 2):
- In the vertical, biases reduced mainly in the top 400m and in the layer 800-2000m.
- The spatial distribution of the bias reduction shows a large impact at the exit of the Labrador Sea, also where the largest bias were found.

Mean corrections to NCEP atmospheric state (Fig. 3):
- Air temperature corrections are dominated by cooling at localized places (e.g., Barents and Labrador Seas; north of the Gulf Stream).
- Precipitation corrections show more precipitation over the Subpolar Gyre and less over the western boundary of the subtropical Atlantic (in particular over the Gulf Stream).
- Wind corrections are important north of 40°N and show two strong cyclonic wind anomalies in the northern north Atlantic (south of the Grand Banks of Newfoundland and in the Icelandic Basin) and an anticyclonic wind anomaly over the Norwegian Sea.

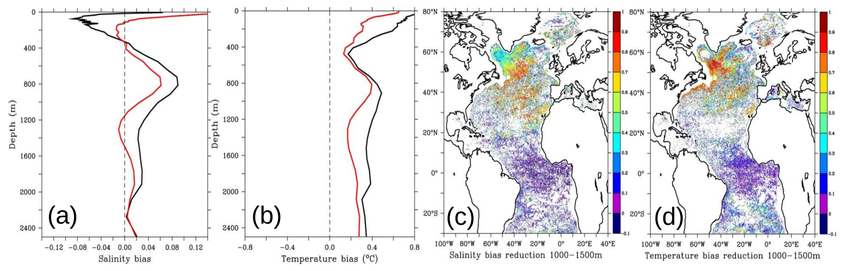

Fig. 2. *Salinity (a) and potential temperature (b) biases from the unconstrained (black) and optimized (red) model integrations. (c,d) Salinity and potential temperature bias reduction in the layer 1000-1500m.*

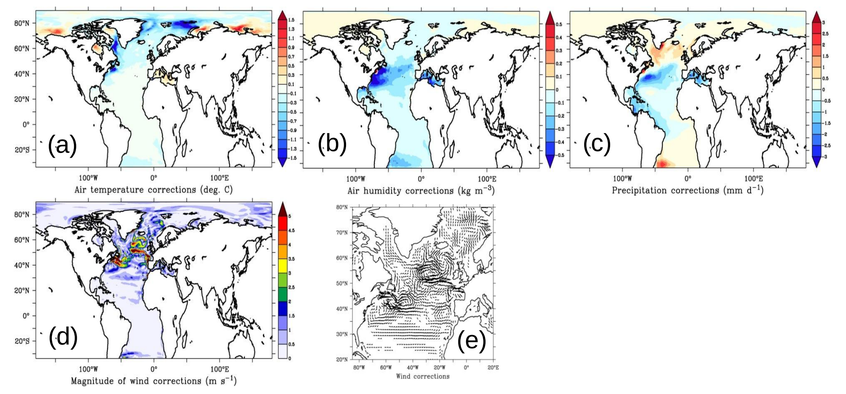

Fig. 3. *Mean corrections to the NCEP atmospheric state: (a) 2m air temperature (b) 2m air humidity, (c) precipitation rate and (d) 10m wind. Panel (e) shows a zoom of the wind (vectors) correction in the North Atlantic.*

3. North Atlantic heat and salt content variability

A pronounced trend in the North Atlantic heat content (HC) is being recorded in recent decades; the synthesis' trends (Fig. 4) are comparable to ARGO-based estimates by Ivchenko et al. 2012. The 0-2000m positive trend slowed during 2001-2002 and 2008, when the upper 100m featured conditions cooler than average. The North Atlantic salt content (SC) also presents positive trends at all levels except at 1000-2000m. Trends have a complex (tripolar) spatial distribution (Fig. 5): positive in Subpolar Gyre and western central Atlantic and negative at the Northwest Corner and eastern boundary upwelling areas.

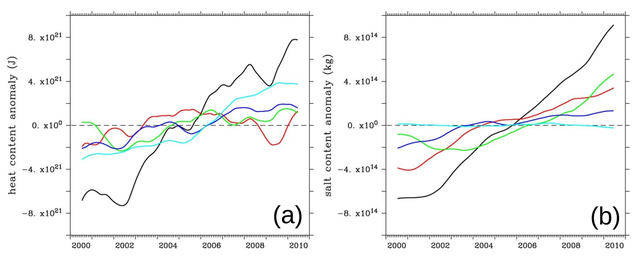

Fig. 4. *North Atlantic (10°N-66°N) integrated (a) HC and (b) SC from the synthesis: 0-2000m (black); 0-100m (red); 100-500m (green); 500-1000m (blue) and 1000-2000m (cyan).*

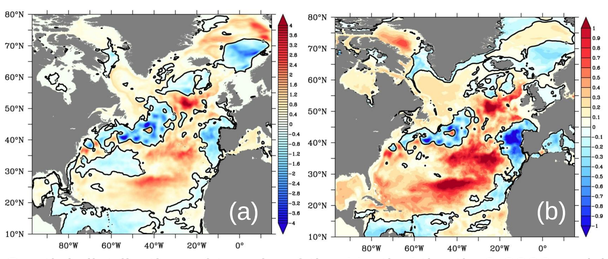

Fig. 5. *Spatial distribution of trends of the North Atlantic 0-2000m: (a) HC (in 10^{18} J/decade) and (b) SC (in 10^{11} kg/decade).*

4. Nordic Seas dense water production and overflows

Time series of simulated overflow transport through the two main Greenland-Iceland-Scotland Ridge (GISR) passages, the Demark St. and the Faroe-Bank Ch. compare remarkably well with observationally-estimated transports (Fig. 6). The seasonal cycles are also comparable, with a tendency for an anti-phase being seen at annual periods. A volume balance (Fig. 7) for the dense layer ($\sigma_\theta \geq 27.8$ kg.m^{-3}), allows an estimate of the 2000-2010 mean dense water produced in the Nordic Seas of about 3.0±0.8 Sv. Its variability is directly transmitted to the dense reservoir but not to the GISR overflows (the latter averaged to 6.0 ±1.0 Sv).

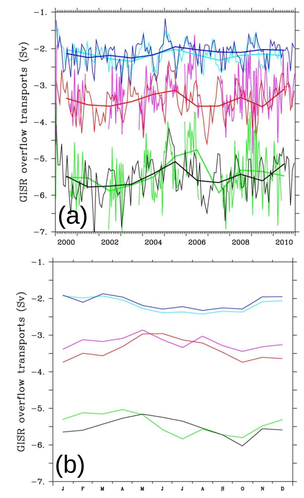

Fig. 6. *Comparison of simulated and observed main GISR overflows (a) and their seasonal cycle (b): Denmark St. (red-synth.; magenta-obs.), Faroe-Bank Channel (blue-synth; cyan-obs.) and their sum (black-synth; green-obs.).*

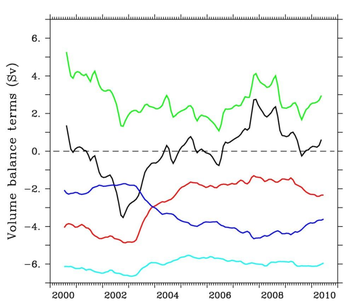

Fig. 7. *Nordic Seas dense water ($\sigma_\theta \geq 27.8$ kg.m^{-3}) volume balance: $\partial V/\partial t$ (black); horiz. convergence (red) and dense water production (green). Also shown are the total Arctic-Nordic Seas exchange (blue) and the total GISR overflow (cyan).*

5. Labrador Sea Water formation and DWBC export

The volumetric estimate of Labrador Sea Water (LSW) formation from the synthesis (Fig. 8a) points to an overall decrease in the analysed period (from 9 to 3 Sv). The export of volume at 45°N (Fig. 8b, cyan) also presents a decrease from the early 2000s until 2009; from mid-2009, a strong export pulse feeds from the LSW pool (Fig. 8a, black). DWBC volume transports at 53°N (Fig. 9) are close to the values reported in observational studies (Fischer et al., 2010).

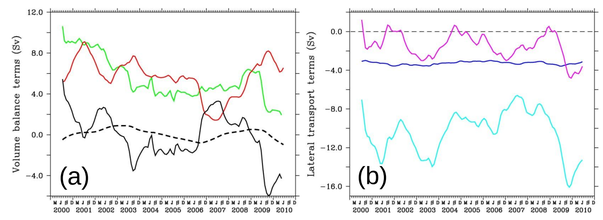

Fig. 8. *(a) Subpolar gyre dense water ($\sigma_\theta \geq 27.68$ kg.m^{-3}) volume balance: $\partial V/\partial t$ (black); horiz. divergence (red) and dense water production (green). (b) Lateral transports contributing to the divergence: northern import at 66°N (blue), western import at 25°W (magenta) and southern export at 45°N (cyan).*

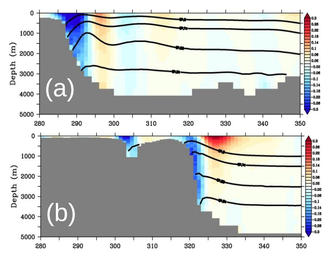

	53°N		47°N	
	DWBC	basin net	DWBC	basin net
surface	-13.4±4.0	17.4±4.0	-22.3±8.2	16.6±4.6
uLSW	-11.1±3.0	-2.8±3.3	-10.0±3.2	-2.9±2.0
dLSW	-14.7±5.1	-6.3±4.2	-13.5±5.7	-7.9±3.5
NEADW	-10.0±3.7	-6.6±3.1	-10.8±4.7	-6.3±3.1
DSOW	-5.2±3.1	-2.9±3.1	-6.6±4.2	0.7±3.2
overt. max.	10.5±1.7		12.1±2.2	

Fig. 9. *Simulated mean meridional velocity at (a) 53°N and (b) 47°N (in m/s). The table summarizes the synthesis 2000-2010 transports (mean±std, in Sv) in relevant layers (based on monthly averages).*

6. Meridional overturning circulation (MOC) and heat transport at 27°N

The MOC at 27°N (and its components) resulting from the synthesis compare very well to the RAPID observational estimates (Rayner et al., 2011), both in their seasonal and inter-annual frequencies (Fig. 10a,b). The MOC shows a pronounced anomaly during 2009/2010. In agreement with McCarthy et al. (2012), the anomaly is partly due to a very low NAO winter in 2009/2010 bringing about wind stress anomalies favourable to a reduction of the northward Ekman transport. More interestingly, the non-ekman upper ocean southward (return) flow shows a longer term transport strengthening (i.e., a MOC decrease). This return flow can be shown to have the same variability as the 1100-5000m deep flow, where the DWBC brings NADW southwards. Fig. 10c shows this transport split into upper and deeper components; most of the signal is due to variability in the layer 3000-5000m.

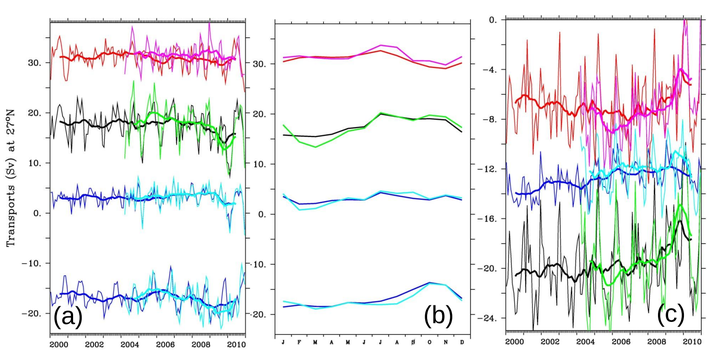

Fig. 10. *(a) Simulated MOC at 27°N (black) decomposed into Florida St. (red), Ekman (blue above) and upper mid-ocean (blue below) transports. RAPID estimates are the shorter time-series superimposed. Panel (b) shows the comparison of the annual climatology derived from both synthesis and observations. (c) Simulated transport in the layer 1100-5000m (black) split into upper (1100-3000m - blue) and lower (3000-5000m - red) components; again the shorter time series are from RAPID.*

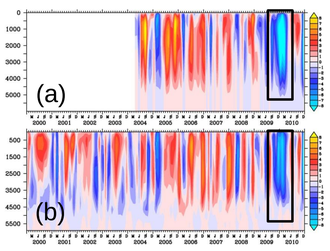

Fig. 11. *Depth-time evolution of (a) observed and (b) simulated anomalies of the vertical cumulative transport (in Sv) at the RAPID section. Black rectangles delimitate the 2009/2010 MOC anomaly,*

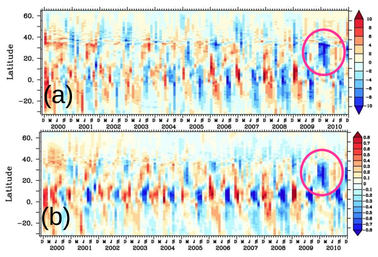

Fig. 12. *Latitude-time evolution of simulated anomalies of (a) maximum overturning streamfunction (in Sv) and (b) meridional heat transport (in PW). Circles enclose the winter 2009/2010 anomaly.*

The synthesis presents a structure of the vertically accumulated transports at 27°N in agreement with RAPID (Fig. 11); the low MOC anomaly at the end of the record is unprecedented in the decade simulated. A latitude-time plot of the MOC maximum from the synthesis (Fig.12a) presents the 2009/2010 anomaly as a single strong event with no apparent unusual connection to the north. The meridional heat transport (cold) anomaly (Fig. 12b) is also confined to the region of MOC anomaly.

Despite the decrease of the 1100-5000m layer transport being consistent with decreasing LSW formation and export via the DWBC further north (Fig. 8), a simple explanation as a propagating pulse along the DWBC is not supported. Instead, the DWBC transport at 27°N is responding to local phenomena inducing NADW re-circulations to the east of the current axis. Fig. 13a shows the complex banded pattern of re-circulations of which the DWBC is part. The structure compares well with in-situ data (Johns et al., 2008). When accumulating transports including the immediate northward recirculation of the DWBC, a regular periodicity of 2-3 years is seen (Fig. 13b).

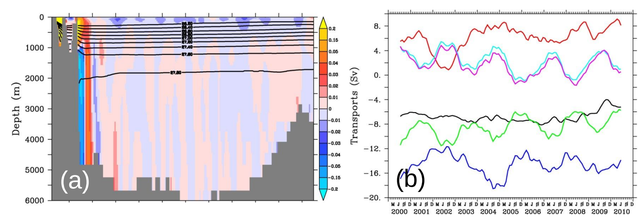

Fig. 13. *(a) 2000-2010 mean meridional velocity (in m/s) at 27°N from the synthesis. (b) Simulated volume transports (in Sv) in the layer 3000-5000m: basin-wide net (black), DWBC (blue), immediate recirculation (red), sum of both (green), interior recirculation until Mid-Atlantic Ridge (cyan) and total interior recirculation (magenta).*

That signal is compensated by an even broader recirculation up to the Mid-Atlantic-Ridge. The regular behaviour of the DWBC+recirc. (or of the interior) is shown to be due to southwestward-propagating Rossby waves, seen in Fig. 14 in the depth anomaly of the σ_θ=27.6 kg.m-3 isopycnal. The waves (reaching deep from the thermocline) have associated zonal currents which enhance/reduce the cyclonic boundary deep recirculation.

The waves do not explain directly the basin-wide integrated signal (which is actually the sum of the entire recirculation) but they are definitely part of the process. Wave interactions with anomalous eddy activity from the Gulf Stream or anomalous Ekman pumping might be at the core of the problem.

These and other processes leading to recirculation in the DWBC are presently being studied with the output from the synthesis.

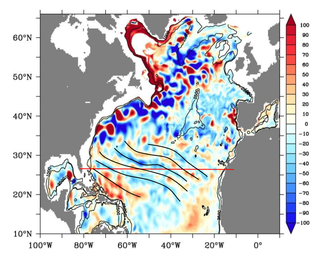

Fig. 14. *Anomaly of the depth of the σ_θ=27.6 kg.m-3 isopycnic surface (in m) during January 2004 from the synthesis. Black curves show crests and troughs of southwestward-propagating waves*

7. Conclusions

A high-resolution ocean synthesis was obtained using the MITgcm adjoint model. After data assimilation, salinity and temperature biases decreased in the top 2000m, in particular in the subpolar gyre. Comparisons between measured and simulated key time-series showed the synthesis to be consistent with in situ measurements (both in terms of mean and variability) at seasonal and inter-annual periods. Four key oceanographic topics were addressed:

- The simulated North Atlantic HC and SC positive trends are consistent with recent ARGO-based estimates by Ivchenko et al. (2012) and vary regionally;
- Dense water overflow at GISR in the synthesis amounts to ~6 Sv, in agreement with observations, as a response to dense water formation in the eastern basins (about 3 Sv), import from the Arctic (2-4 Sv) and/or reservoir changes.
- LSW formation in the synthesis varies from 3 to 9 Sv during the 2000s (mean is 5.5 Sv). The simulated transports of the DWBC at 53°N and 47°N are comparable to measurements summarized by Fischer et al. (2010) and C. Mertens (pers. comm.).
- The simulated MOC at 27°N and its components compare very well to RAPID estimates (Rayner et al., 2011). The very low MOC during winter 2009/2010 (McCarthy et al., 2012) was accompanied by low MHT. The cause was an anomalously weak surface northward Ekman transport superimposed on an enhanced southward upper mid-ocean transport. The latter reflects the DWBC flow, in turn affected by westward propagating Rossby waves.

References
Fischer et al. (2010). Interannual to decadal variability of outflow from the Labrador Sea. *GRL, 37, L24610.*
Ivchenko et al. (2012). Variability of heat and salinity content in the North Atlantic over the last decade. *http://www.noc.soton.ac.uk/ooc/PROJECTS/MONACO*
Johns et al. (2008). Variability of shallow and deep western boundary currents off the Bahamas during 2004-2005. *JPO, 38, 605-623.*
McCarthy et al. (2012). Observed interannual variability of the Atlantic meridional overturning circulation at 26.5°N. *GRL, in press.*
Rayner et al. (2011). Monitoring the Atlantic meridional overturning circulation. *DSR II, 58, 1744-1753.*

Acknowledgments
This work was financially supported by the German Federal Ministry for Education and Research (BMBF) in the frame of project "Nordatlantik". The numerical simulations were performed at the German Climate Computing Center (DKRZ), Hamburg.

Bundesministerium für Bildung und Forschung